NAG-1-210

APPENDIX 4

EFFICIENT LINEAR AND NONLINEAR HEAT CONDUCTION WITH A QUADRILATERAL ELEMENT

BY

WING KAM LIU*

and

TED BELYTSCHKO**

Northwestern University
The Technological Institute
Evanston, Illinois 60201

* Assistant Professor of Mechanical and Nuclear and Civil Engineering.
** Professor of Civil and Mechanical and Nuclear Engineering.

(NASA-CR-170065) EFFICIENT LINEAR AND NONLINEAR HEAT CONDUCTION WITH A QUADRILATERAL ELEMENT (Northwestern Univ.) 38 p HC A03/MF A01 CSCL 20D

N83-20033

Unclas

G3/34 09312

Abstract

A method is presented for performing efficient and stable finite element calculations of heat conduction with quadrilaterals using one-point quadrature. The stability in space is obtained by using a stabilization matrix which is orthogonal to all linear fields and its magnitude is determined by a stabilization parameter. It is shown that the accuracy is almost independent of the value of the stabilization parameter over a wide range of values; in fact, the values 3, 2 and 1 for the normalized stabilization parameter lead to the 5-point, 9-point finite difference and fully integrated finite element operators, respectively, for rectangular meshes and have identical rates of convergence in the L_2 norm. Eigenvalues of the element matrices, which are needed for stability limits, are also given. Numerical applications are used to show that the method yields accurate solutions with large increases in efficiency, particularly in nonlinear problems.

ORIGINAL PAGE IS OF POOR QUALITY

1. INTRODUCTION

Because of the versatility of finite element methods for treating complex geometries and boundary conditions considerable attention has been focused on these methods in heat conduction. One drawback of the finite element method compared to the finite difference method is that presently available formulations tend to be more time consuming. For example, in comparing standard five point or nine point finite difference formulas in two-dimensions with the isoparametric, bilinear quadrilateral with 2x2 quadrature, one finds that in nonlinear heat conduction, a substantial amount of time is used to perform the 2x2 quadrature within each element so that the latter can be markedly slower.

The purpose of this paper is to present techniques through which the bilinear, isoparametric element for two dimensional heat conduction can be used with one point quadrature. Special techniques are needed because when single point quadrature is used, the element matrix contains a spurious singular mode in addition to the singular mode associated with the constant temperature field. For certain boundary conditions, this singular mode leads to singularity of the assembled system matrix, which prevents it from being inverted. While the singularity is absent in the transient system matrix, the presence of the singular modes in the steady-state matrix will lead to oscillatory solutions in which nodal temperatures alternate in sign spatially, and the growth of this mode can lead to uninterpretable results. This is true for both explicit and implicit time integration procedures.

This singular mode is analogous to the hourglass modes found in many finite difference codes for transient analysis of continua [1] and considerable efforts have been devoted to the elimination of these modes in both the finite difference and finite element literature [2-4].

In this paper a stabilization procedure is developed for the quadrilateral element for heat conduction based on the techniques developed in [4] so that one point quadrature can be used effectively; in effect, the spurious singular mode will be eliminated. The procedure is described for both the conductance vector and the element conductance matrices, so that it can be used in both steady-state and transient algorithms with explicit and implicit time integration. As part of this development, the eigenvalues are obtained exactly for both isotropic and anisotropic heat conduction; this should facilitate the choice of a maximum stable time step for explicit time integration and optimal relaxation factors for implicit time integration by iterative equation solvers.

In Section 2, we review the governing equations for linear and nonlinear heat conduction along with the finite element approximations as obtained by a variational principle, which are similar to [5] except that they are written directly for the nonlinear case. Other nonlinear formulations have been given in [6] and [7]. The equations for the one-point quadrature, bilinear, isoparametric quadrilateral are given in Section 3 with the stabilization procedure. Section 4 compares the finite element equations given here to finite difference spatial semidiscretizations based on the standard 5-point and 9-point molecules. An interesting result is that when the mesh is regular, these different molecules can be developed by simply varying the stabilization parameter. The eigenvalues of the element matrices are given in Section 5, whereas the computer implementation of this one point-quadrature for the heat conduction element is given in Section 6.

In Section 7, we present several example problems. The first two examples compare the rate of convergence of this element with 1 point quadrature and with 2 x 2 quadrature of the quadrilateral to show the minor effect of reduced integration on convergence. The remaining problems are transient and are intended to show the improvements in speed which are possible with this element and the difficulties which result when hourglass control is not used; both linear and nonlinear results are presented.

2. GOVERNING EQUATIONS AND VARIATIONAL (WEAK) FORMS

We consider a body Ω enclosed by a surface Γ with unit normal $\underset{\sim}{n}$ which is subdivided into a prescribed θ-surface Γ_θ and a prescribed flux surface Γ_q. We use the following nomenclature

θ	=	temperature
s	=	source per unit volume
q_i	=	heat flux
ρ	=	density
c	=	specific heat
$h(\theta)$	=	convective heat transfer coefficient law
k_{ij}	=	linear conductivity matrix ($k_{ij} = k\delta_{ij}$ for isotropic heat conduction)

The governing equations are:

$$-q_{i,i} + s = \rho c \dot{\theta} \quad \text{in } \Omega \tag{1}$$

$$\theta = \theta^* \quad \text{on } \Gamma_\theta \tag{2}$$

$$-q_i n_i + h(\theta) = q^* \quad \text{on } \Gamma_q \tag{3}$$

$$\theta = \theta_o \quad \text{in } \Omega \text{ when } t = 0 \tag{4}$$

Standard indicial notation is used with repeated subscripts implying a summation. Here a comma designates a partial derivative with respect to x_i, and a superposed dot designates the time (t) derivative.

The completion of Eqs. (1) to (4) also requires a heat-law

$$q_i = f_i(\theta, \theta_{,j}) \tag{5}$$

which for linear heat conduction can be written as

$$q_i = -k_{ij}\, \theta_{,j} \tag{6}$$

The variational or weak form of Eqs. (1) to (4) as given in [8] is

$$m(\theta, v) + r(\theta, v) = f(q, s, v) \tag{7}$$

where v is the test function and

$$m(\theta, v) = \int_\Omega \rho c\, \dot{\theta}\, v\, d\Omega \tag{8}$$

$$r(\theta, v) = -\int_\Omega v_{,i}\, q_i\, d\Omega \tag{9}$$

$$f(q, s, v) = \int_{\Gamma_q} [\, \overset{*}{q} - h(\theta)]v d\Gamma + \int_\Omega s\, v\, d\Omega \tag{10}$$

The finite element equations are obtained by approximating the test functions and the approximate solution for $\theta(\underset{\sim}{x}, t)$ (trial functions) by shape functions N_I. These shape functions are defined in each element, and the approximation in each element is given by using a local separation of variables

$$\theta(\underset{\sim}{x}, t) = \sum_{I=1}^{NODELE} N_I(\underset{\sim}{x})\, \theta_I(t) \tag{11}$$

where θ_I are the nodal values of the temperature and NODELE is the number of nodes in the element. An identical expansion is used for the test function $v(\underset{\sim}{x})$ and the space discretization is performed separately.

The finite element semidiscretization yields the following system of ordinary differential equations for heat conduction

$$\underset{\sim}{M}\,\dot{\underset{\sim}{\theta}} + \underset{\sim}{r} = \underset{\sim}{f} \tag{12a}$$

$$\underset{\sim}{\theta}(0) = \underset{\sim}{\theta}_0 \tag{12b}$$

where $\underset{\sim}{M}$ is obtained from the element matrices $\underset{\sim}{M}^E$ by the standard matrix assembly of finite elements and $\underset{\sim}{r}$ and $\underset{\sim}{f}$ are obtained from the element matrices by vector assembly. The element matrices are given by

$$\underset{\sim}{M}^E = [M_{IJ}]^E = \int_{\Omega^E} \rho c\, N_I\, N_J\, d\Omega \tag{13}$$

$$\underset{\sim}{r}^E = [r_I]^E = -\int_{\Omega^E} N_{I,i}\, q_i\, d\Omega \tag{14}$$

$$\underset{\sim}{f}^E = [f_I]^E = \int_{\Omega^E} N_I\, s\, d\Omega + \int_{\Gamma_q^E} N_I q^* d\Gamma - \int_{\Gamma_q^E} N_I\, h(\theta)\, d\Gamma \tag{15}$$

The above equations are applicable to both linear and nonlinear heat conduction, for $\underset{\sim}{r}$ and $\underset{\sim}{f}$ may be nonlinear in θ. When the conductance k_{ij} is constant, Eq. (12a) can be replaced by

$$\underset{\sim}{M}\,\dot{\underset{\sim}{\theta}} + \underset{\sim}{K}\,\underset{\sim}{\theta} = \underset{\sim}{f} \tag{16}$$

where $\underset{\sim}{K}$ is here called the global conductance matrix, which is assembled from element conductance matrices $\underset{\sim}{K}^E$ given by

$$\underset{\sim}{K}^E = [K_{IJ}]^E = \int_{\Omega^E} N_{I,i}\, k_{ij}\, N_{J,j}\, d\Omega \tag{17}$$

ORIGINAL PAGE IS
OF POOR QUALITY

3. QUADRILATERAL WITH ONE-POINT QUADRATURE

The shape functions for a quadrilateral element are written in a reference plane ξ,η in the form

$$N_I = \frac{1}{4}(1 + \xi_I\,\xi)(1 + \eta_I\,\eta) \tag{18}$$

where ξ_I, η_I are the ξ, η coordinates of node I. If one point quadrature is used, the integrals in Eqs. (13-15) and (17) can be computed by simply evaluating the integrands at $\xi = 0$, $\eta = 0$ and multiplying by the area, i.e. for any function, one-point quadrature gives

$$\int_{\Omega^E} f(\xi,\eta)\, d\Omega = A\, f(0,0) \tag{19}$$

where A is the area of element E.

The following equations then hold on the element level

$$\underset{\sim}{g} = \frac{1}{A}\underset{\sim}{B}\,\underset{\sim}{\theta}^E \tag{20a}$$

$$\underset{\sim}{r}^{E(1)} = \underset{\sim}{B}^T\underset{\sim}{g}(0,0) \tag{20b}$$

and the associated element conductance matrix for linear heat conduction is

$$\underset{\sim}{K}^{E(1)} = \frac{1}{A}\underset{\sim}{B}^T\,\underset{\sim}{D}\,\underset{\sim}{B} \tag{21}$$

where the superscript 1 designates one-point quadrature. Here

$$\underset{\sim}{B} = \begin{Bmatrix} \underset{\sim}{b}_1^T \\ \underset{\sim}{b}_2^T \end{Bmatrix} \tag{22a}$$

$$\underset{\sim}{D} = \begin{bmatrix} k_{11} & k_{12} \\ k_{12} & k_{22} \end{bmatrix} \tag{22b}$$

$$\underset{\sim}{q} = \begin{Bmatrix} q_x \\ q_y \end{Bmatrix} \qquad \underset{\sim}{g} = \begin{Bmatrix} \theta_{,x} \\ \theta_{,y} \end{Bmatrix} \tag{22c}$$

The area of the element, A, is given by

$$A = \frac{1}{2} (x_{31}\, y_{42} + x_{24}\, y_{31}) \tag{23a}$$

and the vectors $\underset{\sim}{b}_i$ are given by

$$\underset{\sim}{b}_1^T = \frac{1}{2} [y_{24}\ y_{31}\ y_{42}\ y_{13}] \tag{23b}$$

$$\underset{\sim}{b}_2^T = \frac{1}{2} [x_{42}\ x_{13}\ x_{24}\ x_{31}] \tag{23c}$$

$$x_{IJ} = x_I - x_J \qquad y_{IJ} = y_I - y_J \tag{23d}$$

For the purpose of identifying the spurious singular mode of $\underset{\sim}{K}^E$ and its control, we will define two additional column vectors

$$\underset{\sim}{s}^T = [1, 1, 1, 1] \tag{24a}$$

ORIGINAL PAGE IS
OF POOR QUALITY

$$\underset{\sim}{h}^T = [1, -1, 1, -1] \qquad (24b)$$

and note that

$$\underset{\sim}{b}_i^T \underset{\sim}{s} = 0 \qquad \underset{\sim}{b}_i^T \underset{\sim}{h} = 0 \qquad \underset{\sim}{s}^T \underset{\sim}{h} = 0 \qquad (24c)$$

These vectors, $\underset{\sim}{b}_i$, $\underset{\sim}{s}$ and $\underset{\sim}{h}$, span the 4 dimensional space of element nodal temperatures and are shown for a typical quadrilateral in Fig. 1.

The linear relationship between nodal sources $\underset{\sim}{r}$ and nodal temperatures $\underset{\sim}{\theta}$ for an element can be written as

$$\underset{\sim}{r}^E = \underset{\sim}{K}^{E(1)} \underset{\sim}{\theta}^E \qquad (25a)$$

$$= \frac{1}{A} (\underset{\sim}{b}_i \, k_{ij} \, \underset{\sim}{b}_j^T) \; \underset{\sim}{\theta}^E \qquad (25b)$$

If we let $\underset{\sim}{\theta}^E = \underset{\sim}{s}$ or $\underset{\sim}{\theta}^E = \underset{\sim}{h}$, , the orthogonality properties, Eq. (24c) immediately lead to the result that $\underset{\sim}{r}^E = \underset{\sim}{0}$. Therefore, these two sets of nodal temperatures correspond to singular modes of the element matrix $\underset{\sim}{K}^{E(1)}$. The first, $\underset{\sim}{\theta}^E = \underset{\sim}{s}$, is expected and necessary since it corresponds to a constant temperature field; if a stiffness does not give $\underset{\sim}{r}^E = \underset{\sim}{0}$ for this mode it will not be convergent. We will call this the proper null-space of $\underset{\sim}{K}^{E(1)}$. The second, $\underset{\sim}{\theta}^E = \underset{\sim}{h}$, is undesirable and often is called a spurious singular mode, since it can lead to singularity of the assembled finite element equations. The presence of an additional singular mode is often called a "rank deficiency" of the element matrix. Note that the two vectors

$\underset{\sim}{h}$ and $\underset{\sim}{s}$ span the null-space of the element matrix.

To eliminate this singular mode, we augment the element conductance matrix by a stabilization matrix [9].

$$\underset{\sim}{K}^E = \underset{\sim}{K}^{E(1)} + \underset{\sim}{K}^E_{stab} \tag{26}$$

where the stabilization matrix is given by

$$\underset{\sim}{K}^E_{stab} = \bar{\varepsilon}\, \underset{\sim}{\gamma}\, \underset{\sim}{\gamma}^T \tag{27}$$

The choice of the constant $\bar{\varepsilon}$ will be described later.

This stabilization matrix is obtained by defining an additional generalized thermal gradient $\tilde{g}$ and flux $\tilde{q}$ by

$$\tilde{g} = \underset{\sim}{\gamma}^T \underset{\sim}{\theta}^E \tag{28}$$

$$\tilde{q} = \bar{\varepsilon}\, \tilde{g} \tag{29}$$

This generalized gradient and flux are added to compensate for the contribution to $r(\theta, v)$ which is lost due to one point quadrature, so in effect we now have instead of Eq. (9) that on an element level

$$r^E(\theta, v) = \int_{\Omega^E} v_{,i}\, q_i\, d\Omega - \tilde{g}(v)\, \tilde{q} \tag{30}$$

$$= \underset{\sim}{v}^T \underset{\sim}{r}^{E(1)} + \underset{\sim}{v}^T \underset{\sim}{\gamma}\, \tilde{q} \tag{31}$$

Thus the element nodal sources are given by

$$\underset{\sim}{r}^E = \underset{\sim}{r}^{E(1)} + \chi \tilde{q} \tag{32}$$

and Eq. (27) follows immediately from (32) and (28).

The form of χ will be chosen so that the following conditions are met:

i. for any vector of nodal displacements which is defined by a linear (or constant) temperature field, $\tilde{g} = 0$ in Eq. (28);

ii. for any other set of nodal temperatures, $\tilde{g} \neq 0$.

To put this into more precise terms, we designate the vector space of nodal temperatures of an element by R^4 and the null-space of χ by $R_0^{4\gamma}$. Since the 4 vectors $\underset{\sim}{b}_1$, $\underset{\sim}{b}_2$, $\underset{\sim}{s}$ and $\underset{\sim}{h}$ are linearly independent, they span R^4. As χ is in R^4 , we can expand it in terms of these base vectors as follows

$$\chi = a_1 \underset{\sim}{b}_1 + a_2 \underset{\sim}{b}_2 + a_3 \underset{\sim}{s} + a_4 \underset{\sim}{h} \tag{33}$$

An arbitrary linear temperature field is given by

$$\theta\ (x, y) = c_1\ x + c_2\ y + c_3 \tag{34}$$

and substituting in the nodal values we obtain the following expression for nodal temperatures

$$\underset{\sim}{\theta}^E = c_1 \underset{\sim}{x} + c_2 \underset{\sim}{y} + c_3 \underset{\sim}{s} \tag{35a}$$

where

$$\mathbf{x}^T = (x_1, x_2, x_3, x_4) \tag{35b}$$

$$\mathbf{y}^T = (y_1, y_2, y_3, y_4) \tag{35c}$$

We note the following identity from [4]

$$\mathbf{x}_i^T \mathbf{b}_j = A\,\delta_{ij} \qquad (\mathbf{x}_1 \equiv \mathbf{x},\ \mathbf{x}_2 \equiv \mathbf{y}) \tag{36}$$

which is easily verified by simply substituting in the values of $\mathbf{b}_i$ and A.

The first condition then requires that $\tilde{g}$ (given by Eq. (28)) must vanish for all $\boldsymbol{\theta}^E$ i.e.

$$(a_1 \mathbf{b}_1^T + a_2 \mathbf{b}_2^T + a_3 \mathbf{s}^T + a_4 \mathbf{h}^T)\,(c_1 \mathbf{x} + c_2 \mathbf{y} + c_3 \mathbf{s}) = 0 \qquad \text{for all } c_i \tag{37}$$

Using the orthogonality of $\mathbf{s}$ and $\mathbf{h}$ and, their orthogonality with $\mathbf{b}_i$, and Eq. (36) then yields

$$\boldsymbol{\gamma} = \frac{1}{A}\,[A\,\mathbf{h} - (\mathbf{h}^T \mathbf{x})\,\mathbf{b}_1 - (\mathbf{h}^T \mathbf{y})\,\mathbf{b}_2] \tag{38}$$

We will call the vector $\mathbf{s}_1$ the proper null-space of R^4; its complement is of dimension 3.

Since $\boldsymbol{\gamma}$ is linearly independent of $\mathbf{b}_i$, the 3 together must span the entire complement of the proper null-space of R^4, so the second condition is satisfied.

It is of interest to note that the complements of the null-spaces of $\underset{\sim}{K}^{E(1)}$ and of $\underset{\sim}{K}^{E}_{stab}$ (the latter coincides with that of γ) are not exclusive; i.e. the intersections of those spaces is not empty. This means that $\underset{\sim}{K}^{E}_{stab}$ will affect the solution if it is not linear and the elements are not rectangular. Nevertheless, the stabilization matrix does not affect linear or constant fields, so it should not deleteriously affect convergence; though this remains to be proven, the numerical results in Section 7 confirm this fact.

The stiffness matrix with the stabilization can be written as

$$\underset{\sim}{K}^{E} = \frac{1}{A}\, \underset{\sim}{b}_{i}\, \bar{k}_{ij}\, \underset{\sim}{b}^{T}_{j} + \bar{\varepsilon}\, \underset{\sim}{h}\, \underset{\sim}{h}^{T} \qquad (39)$$

1 not "ℓ"

where

$$\bar{k}_{ij} = k_{ij} + \bar{\varepsilon} A(\underset{\sim}{h}^{T}\underset{\sim}{x}_{i})\;(\underset{\sim}{h}^{T}\underset{\sim}{x}_{j}) \qquad (40)$$

and

$$\bar{\varepsilon} = \frac{k_{ii}(\ell_x^2 + \ell_y^2)}{24A} \qquad (41a)$$

or

$$\bar{\varepsilon} = \frac{k\,(\ell_x^2 + \ell_y^2)}{12A} \qquad (41b)$$

where ℓ_x and ℓ_y are the lengths of the sides of the element.

4. COMPARISON WITH FINITE DIFFERENCE FORMULAS AND OTHER FINITE ELEMENTS

For rectangular and square arrangements of meshes, it is possible to compare this finite element with standard finite difference formulas and fully integrated quadrilateral finite elements. These comparison help in assessing the role of the stabilization parameter ε and the lack of sensitivity of solutions to its value.

For a square finite difference mesh, the 5 point and a 9 point molecule [10] are given in Table 1. The complete stiffness (1-point quadrature plus stabilization) is also given for $\varepsilon = 3$ and $\varepsilon = 2$. It can be shown by the simple assembly of the finite element equations that

i. $\varepsilon = 3$ corresponds to the 5-point molecule

ii. $\varepsilon = 2$ corresponds to the 9-point molecule

It can also be shown that as defined in Eq. (41), the value of $\varepsilon = 1$ gives the fully integrated finite element stiffness; while $\varepsilon = 0$ of course corresponds to the 1 point quadrature stiffness. Thus commonly used finite difference and element formulas are associated with a large range of ε values.

5. EIGENVALUE ANALYSIS OF ELEMENT

We consider the following form of the eigenvalue problem

$$\underset{\sim}{K}^E \; \underset{\sim}{\theta}^E = \lambda^E \; \underset{\sim}{M}^E \, \underset{\sim}{\theta}^E \qquad (42)$$

where $\underset{\sim}{M}^E$ is the lumped element capacitance matrix, which is given by

$$\underset{\sim}{M}^E = \rho c \, \underset{\sim}{I} \qquad (43)$$

where $\underset{\sim}{I}$ is the identity matrix. The system is associated with the eigenvalue problem

$$\underset{\sim}{K} \; \underset{\sim}{\theta} = \lambda \; \underset{\sim}{M} \, \underset{\sim}{\theta} \qquad (44)$$

and according to [12], the largest eigenvalue of any individual element will bound the maximum frequency from above, so

$$\lambda_{max} < \max_{\text{for all } E} \lambda^E_{max} \qquad (45)$$

Since the stability of Euler integration requires that

$$\Delta t < \frac{2}{\lambda_{max}} \qquad (46)$$

a time step chosen by

$$\Delta t = \min_{\substack{\text{for all} \\ E}} \frac{2}{\lambda^E_{max}} \qquad (47)$$

will automatically be stable.

In order to obtain the eigenvalues for Eq. (42), we note that the element stiffness as given by Eq. (39) is the sum of 2 terms and the eigenvectors of the two terms can be constructed as follows:

1. The two nonzero eigenvectors of the first term on the right hand side of Eq. (39) are linear combinations of $\underset{\sim}{b}_1$ and $\underset{\sim}{b}_2$, and since $\underset{\sim}{b}_1$ and $\underset{\sim}{b}_2$ are in the null-space of the second term, this will also be an eigenvector of $\underset{\sim}{K}^E$.

2. The nonzero eigenvector of the second term is $\underset{\sim}{h}$ and, since $\underset{\sim}{h}$ is in the null-space of the first term, it is an eigenvector of $\underset{\sim}{K}^E$.

The maximum eigenvalue of Eq. (42) can be then be shown to be given by

$$\lambda^E_{max} = \frac{\alpha}{A^2} \max \{ X + Y \pm \sqrt{(X-Y)^2 + 4Z^2} \, , \, 16 \bar{\varepsilon} A^2 / k \} \quad (48)$$

where

$$\begin{aligned} \alpha &= k/\rho c \\ X &= \bar{K}_{ij} \; B_{1i} \; B_{1j} \\ Y &= \bar{K}_{ij} \; B_{2i} \; B_{2j} \\ Z &= -\bar{K}_{ij} \; B_{1i} \; B_{2j} \end{aligned} \quad (49)$$

The following special cases are of interest:

1. If the material is isotropic and the element rectangular

$$\lambda^E_{max} = \frac{4\alpha}{\ell^2_{min}} \quad (50)$$

where ℓ_{min} is the minimum element length, provided that

$$\epsilon < \frac{3r^2}{1+r^2} \tag{51}$$

where r is the ratio of the lengths of long side to the short side. This, with Eq.(47), yields the following condition for stability

$$\Delta t < \frac{\alpha \ell_{min}^2}{2} \tag{52}$$

ii. For square meshes with a distance ℓ between nodes and with $\epsilon > \frac{3}{2}$, the maximum eigenvalue is given by the second term in Eq. (48), i. e.

$$\lambda_{max}^E = \frac{8\epsilon\alpha}{3\ell^2} \tag{53}$$

Remark 1. The eigenvalue in Eq. (53) governs the time step for the 5-point and 9-point difference formulas (ϵ = 3 and 2 respectively), so the stable time step for these difference formulas is smaller than for the finite element method. This contrasts with the findings in [11] and [12], where the opposite was found because (1) less accurate bounds were used for the eigenvaules and (2) the consistent capacitance matrix was used.

Remark 2. The stability limit for the time step resulting from Eq. (53) for the 5-point difference formula (ϵ = 3), agrees exactly with the result of a Neumann analysis given in (13)

$$\Delta t < \frac{\ell^2}{4\alpha} \tag{54}$$

by title, all "u c"

ORIGINAL PAGE IS OF POOR QUALITY

6. Explicit Integration Using One Point Quadrature and Hourglass Control For Quadrilaterals

For simplicity, we have dropped the superscript E in this section. We first define explicitly the one point quadrature element vector $\underset{\sim}{r}^{(1)}$ and the stabilization element vector $\underset{\sim}{r}^{h}$ employing hourglass control. Then the one point quadrature with hourglass control element vector $\underset{\sim}{r}$ is equal to the sum of $\underset{\sim}{r}^{(1)}$ and $\underset{\sim}{r}^{h}$.

One Point Integration

As give in eq. (14), the element vector $\underset{\sim}{r}$ is:

$$r_I = -\int_\Omega \left(N_{I,x}\, q_x + N_{I,y}\, q_y\right) d\Omega \tag{55}$$

where q_x and q_y are (see Eq. (22c)):

$$q_x = -\left(k_{11} g_x + k_{12} g_y\right) \tag{56a}$$

$$q_y = -\left(k_{12} g_x + k_{22} g_y\right) \tag{56b}$$

and

$$g_x = \frac{1}{2A}\left[\, y_{24}\left(\theta_1 - \theta_3\right) + y_{31}\left(\theta_2 - \theta_4\right)\right] \tag{56c}$$

$$g_y = \frac{1}{2A}\left[\, x_{42}\left(\theta_1 - \theta_3\right) + x_{13}\left(\theta_2 - \theta_4\right)\right] \tag{56d}$$

Employing one point integration

$$r_I^{(1)} = b_{1I} q_x + b_{2I} q_y = b_{iI} q_i \tag{57}$$

ORIGINAL PAGE IS
OF POOR QUALITY

where b_{1I} and b_{2I} are defined in eqs. (23b) and (23c) respectively.

Hourglass Control

The stabilization vector as defined in eq. (32) is:

$$\underset{\sim}{r}^h = \underset{\sim}{\gamma}\tilde{q} \tag{58}$$

where

$$\tilde{q} = \bar{\varepsilon}\,\tilde{g} \tag{59}$$

and

$$\tilde{g} = \frac{1}{2}\left[(\theta_1 - \theta_2 + \theta_3 - \theta_4) - (g_x a_x + g_y a_y)\right] \tag{60a}$$

$$a_x = x_1 - x_2 + x_3 - x_4 \tag{60b}$$

$$a_y = y_1 - y_2 + y_3 - y_4 \tag{60c}$$

The nodal components of this hourglass vector are:

$$r_I^h = h_I\tilde{q} - \frac{1}{A}\, b_{iI}x_{iJ}h_J\tilde{q} \tag{61}$$

Therefore the element vector using one point quadrature and hourglass control for a quadrilateral is:

$$r_I = h_I \tilde{q} - \frac{1}{A} b_{iI} x_{iJ} h_J \tilde{q} + b_{iI} q_i \tag{62}$$

After some algebra one can show that

$$r_I = b_{1I} q_x^* + b_{2I} q_y^* + h_I \tilde{q} \tag{63}$$

where

$$q_x^* = q_x - \frac{1}{A} a_x \tilde{q} \tag{64a}$$

and

$$q_y^* = q_y - \frac{1}{A} a_y \tilde{q} \tag{64b}$$

7. Numerical Results

A two dimensional finite element pilot computer code incorporating the methodologies described in the previous sections has been written to evaluate the performance of this one point quadrature element and our critical time step estimates. Four numerical examples are presented to demonstrate the accuracy, stability criterion and efficiency of these proposed methods. Results are compared with exact solutions or approximate solutions using two by two quadrature. All computations are performed on a CDC Cyber 170/730 computer in single precision (60 bits per floating point word). For the transient analysis, a lumped capacitance matrix is used and the predictor-corrector explicit algorithms with $\alpha = 0.5$ used in [8] are employed to carry out the time integration.

Example 1: Convergence Study of a Unit Square Plate with Prescribed Temperatures

Due to symmetry of the geometry and prescribed temperatures, only half of the unit square plate is modelled with 32 (4 x 8), 128 (8 x 16) and 200 (10 x 20) elements respectively. These three finite element meshes are depicted in Fig 2. Side BC is a line of symmetry (insulated). Sides AD and DC are prescribed a constant uniform temperaure of 0.0, while sides AB is prescribed with a constant temperature distribution of sin πx where the x-axis is defined by joining node A to node B. Hence the temperatures at nodes A and B are 0.0 and 1.0 respectively. The exact steady-state solution is given by:

$$\theta^{exact}(x,y) = \sinh \pi (1.0-y) \sin \pi x / \sinh \pi$$

Two values of the stabilization parameter ε were tested. For $\varepsilon = 1.0$, this element is identical to the two by two quadrature element (since the elements are rectangular); whereas for $\epsilon = 0.0$, it is identical to the one point quadrature element. The temperature profiles along BC obtained from these three finite element meshes (with $\epsilon = 1.0$) and from the analytical solution are also despicted in Fig.2. The finite element solutions of the case $\epsilon = 0.0$ differ from those of the case $\epsilon = 1.0$ in the third or fourth digit. Therefore they are not plotted. As can be seen, the finite element solutions are virtually identical to the exact solution.

We also computed the L_2 error norm for these solutions as follows:

$$E = \{ \int_A e^2 dA \}^{1/2}$$

where $e = \theta^{exact} - \theta^{FEM}$ and A is the area. The total L_2 error, E, is computed using a 5 x 5 quadrature in each element. We obtained convergence rates of 1.899, 1.908 and 1.930 for the cases of $\epsilon = 2.0$, 1.0 and 0.0, respectively, which agree reasonably with the theoretical convergence rate of 2.

<u>Remark 1.</u> The reduction of the quadrature rule from 2 x 2 to 1 has no significant effect on the convergence rate.

<u>Remark 2.</u> It is possible to solve this problem with the stabilization parameter $\epsilon = 0$ because the boundary conditions eliminate the rank deficiency of the assembled mesh. This is not always possible, as will be seen subsequently.

<u>Remark 3.</u> The convergence rate of the 9 point Laplacian ($\epsilon = 2.0$), which has a much smaller truncation error, shows no improvement over the finite element method.

<u>Example 2:</u> <u>Convergence Study of a Circular Plate with a Heat Source</u>

Due to double symmetry, only a quarter of the circular plate (which is heated with a uniform constant heat source (S = 1.0) is modelled with 12, 48 and 192 elements respectively. The finite elements meshes are shown in Fig. 3. It should be observed that some of the quadrilateral elements are quite skewed. The exact solution for this circular plate with radius $r = 5.0$, thermal conductivity $k = 0.04$ and a constant temperature of 0.0 at $r = 5.0$ is given as:

$$\theta^{Exact}(r) = 6.25\,(25 - r^2)$$

As in the preceding example, two values of the stabilization parameter of 1.0 and 0.0 respectively are tested. However, due to the skewness of the elements, the $\epsilon = 1.0$ elements are not the same as the two by two quadrature elements. The $\epsilon = 0.0$ elements are still identical to the one point quadrature elements. The temperature profiles along nodes 1 to 45 obtained from these three finite element meshes (with $\epsilon = 1.0$) and the exact solution are also despicted in Fig. 3. Again, we found that the finite element solutions of the case $\epsilon = 0.0$ differ from those obtained using $\epsilon = 1.0$ in the third or fourth digit. Therefore they are not plotted. The pointwise convergence of this stabilized element is cleared shown in the plot.

We obtained convergence rates of 1.955 and 1.924 for the cases of $\epsilon = 1.0$ and 0.0 respectively which agree well with the expected convergence rate of 2.0.

Example 3: Linear Transient Thermal Analysis of a Wedge

The problem statement is depicted on the top of Fig.4. The finite element mesh consists of 100 elements and 121 nodes. The thermal diffusivity of the wedge is 0.001. The initial temperature for all the nodes is 0.1. All four sides are insulated. The heat load which is also shown in Fig. 4 is applied at node 1. A constant time step of 1.0 is used for this problem. This time step is computed according to Eq. (48). The temperature-time histories at four different locations are presented also in Fig. 4. These results are obtained using ϵ = 1.0 stabilized element. These results are virtually identical to those obtained using two by two quadrature elements. For values of ϵ = 0.8 and 1.2, the peaks at node 1 are about 4% below and 4% above the solution with 2 x 2 quadrature, therefore ϵ = 1.0 is recommended.

Example 4: Linear and Nonlinear Transient Thermal Analysis of a Circular Plate

The "medium" finite element mesh (48 elements with no heat source) shown in Fig. 3 is employed for this problem. The heat load which is shown in Fig. 4 is applied at node 1. The initial temperature for all the nodes is 0.1. All boundaries are insulated. The thermal diffusivity of the plate is 0.004. According to Eq. 48, it corresponds to a critical time step of 1.0. Two hundred time steps are run (at the critical time step) to obtain the temperature-time histories shown in Fig. 5a. These results are obtained using ϵ = 1.0 and the solutions are virtually identical to those obtained using two by two quadrature elements. However, we obtained severe spatial oscillatory solutions using ϵ = 0.0 for this problem (see Fig. 5b).

In order to demonstrate the effectiveness of this one point quadrature element with stabilization, the thermal diffusivity, a, is changed to:

$$a = 0.004\,(1.0 + 0.01\theta)$$

to make the problem nonlinear. A constant time step of 0.2 is used for this nonlinear problem. The computed solution using ϵ = 1.0 are also presented in Fig. 5a. These results are almost the same as those using two-by-two-quadrature elements except there is a 3% difference in the peak temperature of node 1. However, we gain a factor of 4.38 in solution time by employing the stabilized one-point element as compared to 2 x 2 quadrature. Although a factor of 4.0 would be expected, the savings are actually greater because the shape functions need not be evaluated at quadrature points in this procedure.

8. CONCLUSIONS

In this paper, an efficient computational method has been developed for the linear and nonlinear heat conduction with a quadrilateral element. A computationally-useful method of estimating the critical time step for this element in explicit time integration is given. The computer implementation aspects as well as the evaluation of the performance of this new element as applied to two-dimensional steady and transient thermal analysis are also presented.

Numerical results show:

(1) this method yields accurate solutions,

(2) the great increase in computational efficiency especially in nonlinear analysis, and

(3) the importance of this method as applied to three dimensional and/or nonlinear thermal analysis.

Comparison with finite difference formulas has shown that various values of the stabilization parameter, the 5-point and 9-point molecules can be obtained. The convergence rate, however, appears to be independent of ϵ which means it is independent of the order of quadrature in the finite element method.

Acknowledgment

The senior author would like to acknowledge his support under NASA Grant NAG-1-210. The support of Ted Belytschko by Air Force Office of Scientific Research Grant F49620-82-K0013 is gratefully acknowledged.

We wish to acknowledge the assistance of Edward Law in obtaining computer result for this paper.

ORIGINAL PAGE IS OF POOR QUALITY

REFERENCES

1. G. Maenchen and S. Sack, "The Tensor Code" in Methods in Computational Physics , Vol. 3, ed. by B. Alder, et al., Academic Press, 1964, pp. 181-210.

2. A. G. Petschek and M. E. H. Hanson, "Difference Equations for Two-Dimensional Elastic Flow", Journal of Computational Physics, Vol. 3, pp. 307-321, 1968.

3. T.B. Belytschko, "Finite Element Approach to Hydrodynamics and Mesh Stabilization" in Computational Methods inn Nonlinear Mechanics, ed. by J.T.Oden, et al., the Texas Institute for Computational Mechanics, 1974.

4. D. P. Flanagan and T. B. Belytschko, "A Uniform Strain Hexahedron and Quadrilateral with Orthogonal Hourglass Control", International Journal Numerical Methods in Engineering, Vol. 17, 1981, pp. 679-706.

5. E. L. Wilson and R. E. Nickell, " Application of the Finite Element Method to Heat Conduction Analysis". Nuclear Engineering and Design, Vol. 4, 1966, pp. 276-286.

6. C. A. Ramirez and J. T. Oden, "Finite Element Technique Applied to Heat Conduction in Solids with Temperature Dependent Thermal Conductivity", International Journal Numerical Methods in Engineering Vol. 7, 1973, pp. 345-355.

7. G. Comini, S. D. Jindice, R. W. Lewis and O. C. Zienkiewicz, "Finite Element Solution of Nonlinear Heat Conduction with Special Reference to Phase Change", International Journal Numerical Methods in Engineering, Vol. 8, 1974, pp. 613-624.

8. W. K. Liu, "Development of Mixed Time Partition Procedures for Thermal Analysis of Structures", to appear in International Journal Numerical Methods in Engineering, 1982.

9. T. B. Belytschko, C. S. Tsay and W. K. Liu, "A Stabilization Matrix for the Bilinear Mindlin Plate Element", Computer Methods in Applied Mechanics and Engineering, Vol.29, 1981, pp. 313-327.

10. F. H.Hildebrand, " Finite Difference Equations and Simulations", Prentice-Hall, Inc., Englewood-Cliffs, New Jersey, 1968, p. 253.

11. R.V.S. Yalamanchili and S. C. Chu, "Stability and Oscillation Characteristics of Finite-Element, Finite-Difference, and Weighted-Residuals Methods for Transient Two-Dimensional Heat Conduction in Solids", Journal of Heat Transfer, May, 1973, pp. 235-239.

12. G. E. Myers, "The Critical Time Step for Finite Element Solutions for Two Dimensional Heat Conduction Transients", Journal of Heat Transfer,Feb., 1978, pp. 120-127.

13. R. Richtmyer and K.W. Morton, "Difference Methods for Initial Value Problems", Interscience Publishers, New York, 1967.

TABLE 1

Relationship between stabilization parameter ε and finite difference formulas square mesh

ε	$\underset{\sim}{K}^E$	Difference Molecule
		5-point
3	$\frac{k}{2}\begin{bmatrix} 2 & -1 & 0 & -1 \\ -1 & 2 & -1 & 0 \\ 0 & -1 & 2 & -1 \\ -1 & 0 & -1 & 2 \end{bmatrix}$	$\begin{array}{ccc} & 1 & \\ 1 & -4 & 1 \\ & 1 & \end{array}$
		9 point, Ref. [10]
2	$\frac{k}{6}\begin{bmatrix} 5 & -2 & -1 & -2 \\ -2 & 5 & -2 & -1 \\ -1 & -2 & 5 & -2 \\ -2 & -1 & -1 & 5 \end{bmatrix}$	$\frac{1}{6}\left(\begin{array}{ccc} 1 & 4 & 1 \\ 4 & -20 & 4 \\ 1 & 4 & 1 \end{array}\right)$
1	$\frac{k}{6}\begin{bmatrix} 4 & -1 & -2 & -1 \\ -1 & 4 & -1 & -2 \\ -2 & -1 & 4 & -1 \\ -1 & -2 & 1 & 4 \end{bmatrix}$	$\frac{1}{6}\left(\begin{array}{ccc} 2 & 2 & 2 \\ 2 & 16 & 2 \\ 2 & 2 & 2 \end{array}\right)$

FIGURE CAPTIONS

Fig. 1 Base Vectors for a typical quadrilateral.

Fig. 2 Convergence study of a Unit Square plate with Prescribed Temperatures.

Fig. 3 Convergence study of a circular plate with a heat source.

Fig. 4 Linear transient thermal analysis of a wedge.

Fig. 5 Linear and Nonlinear Transient Thermal Analysis of a Circular Plate (a) results obtained with the stabilization matrix (b) oscillatory solutions obtained without the stabilization matrix.

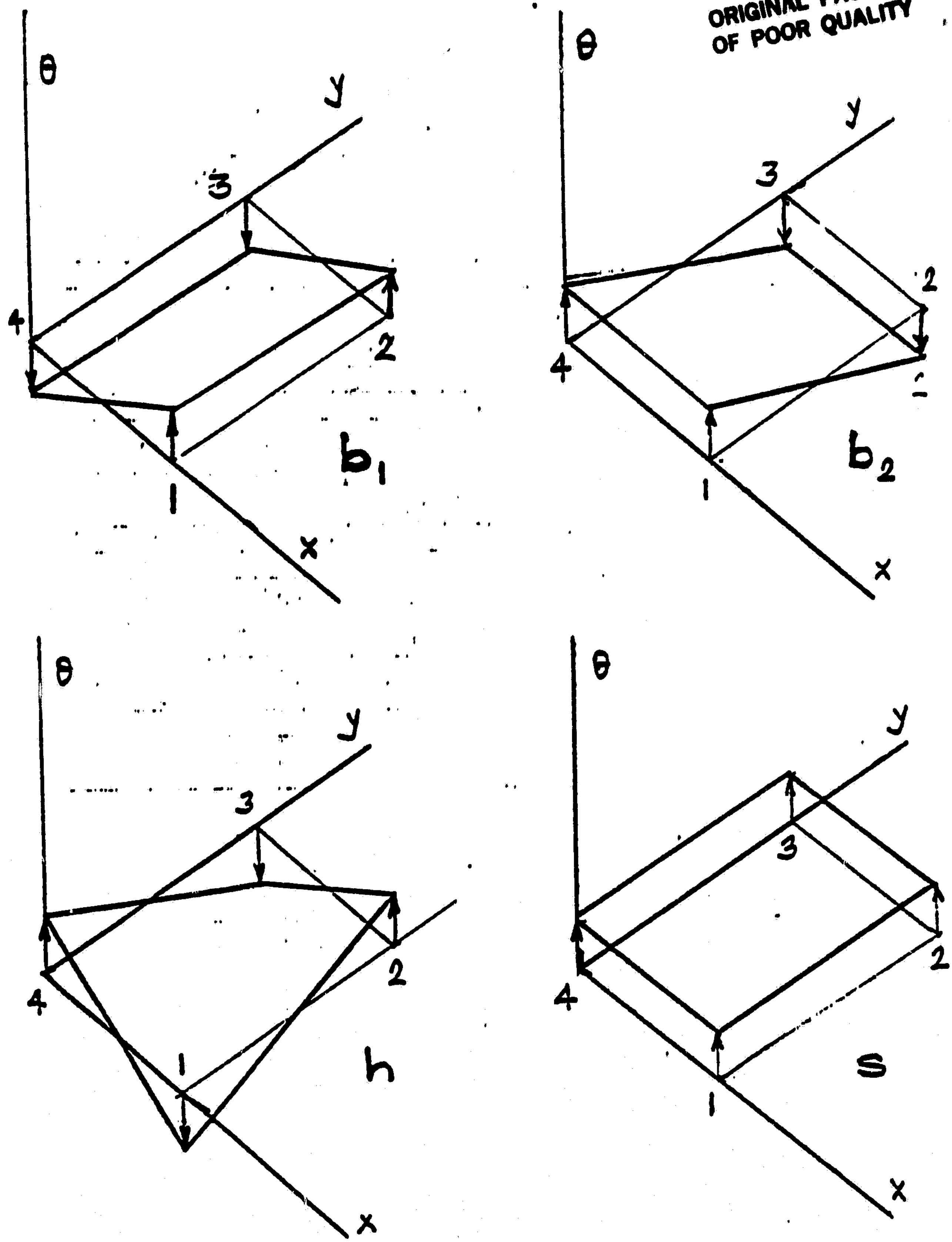

Fig. 1

Fig 2

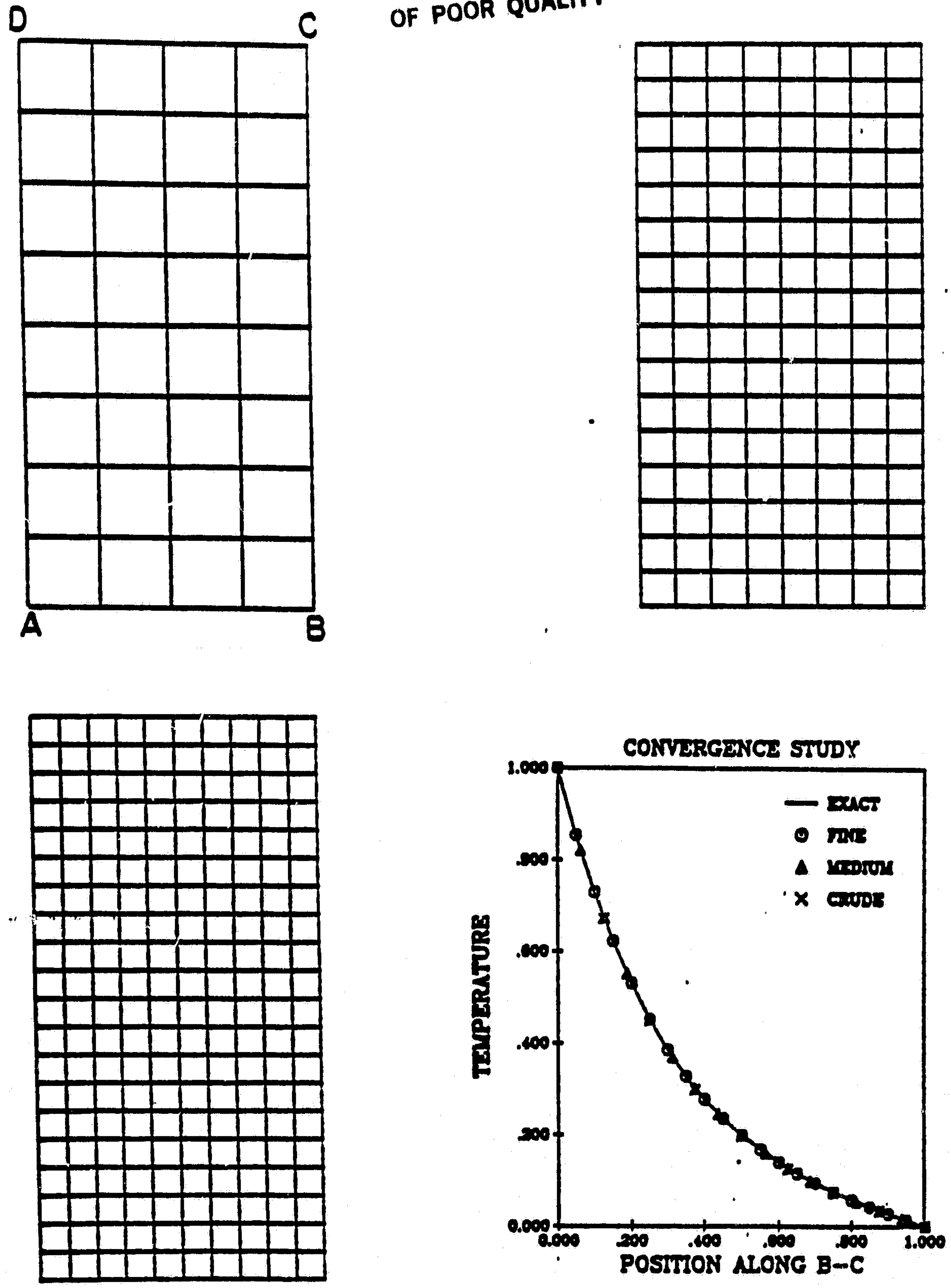
D
C
A
B
CONVERGENCE STUDY
EXACT
FINE
MEDIUM
CRUDE
TEMPERATURE
1.000
.800
.600
.400
.200
0.000
0.000
.200
.400
.600
.800
1.000
POSITION ALONG B--C

Fig 2

Fig 3

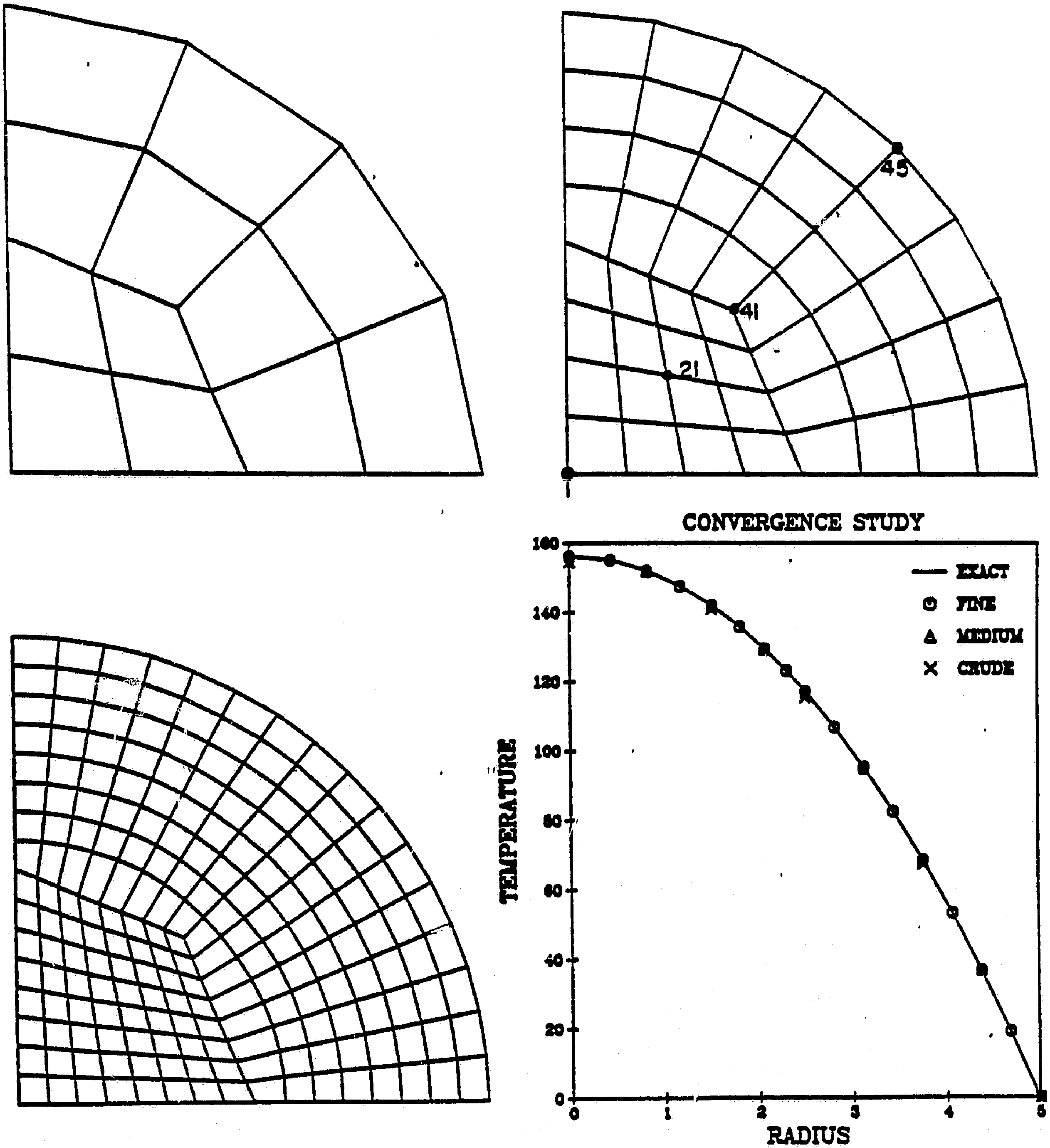
45
41
21
1
CONVERGENCE STUDY
160
140
120
100
80
60
40
20
0
TEMPERATURE
0
1
2
3
4
5
RADIUS
EXACT
FINE
MEDIUM
CRUDE

Fig 3

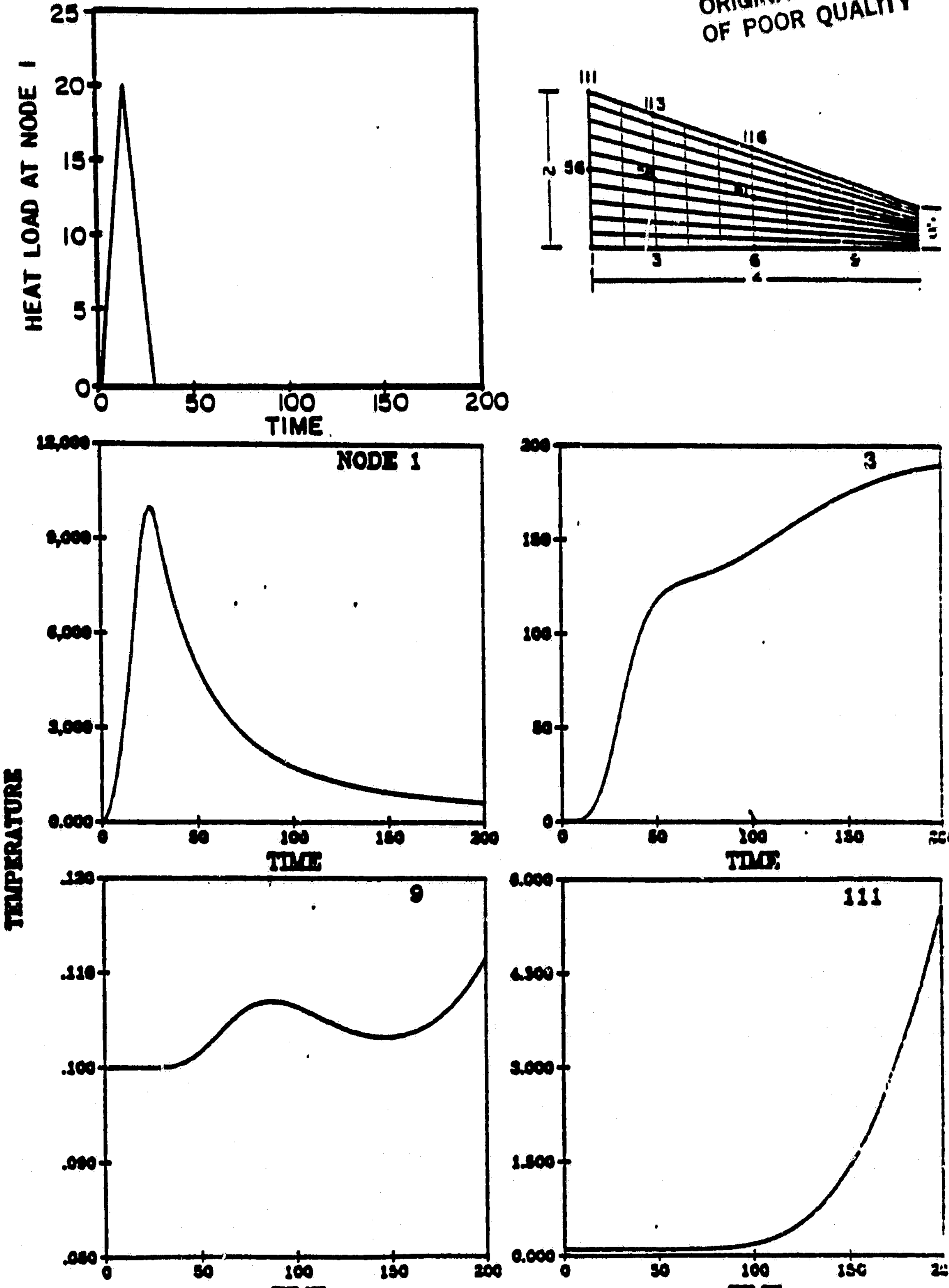
HEAT LOAD AT NODE 1
TIME
0
50
100
150
200
0
5
10
15
20
25
111
113
116
56
3
6
9
1
2
4
NODE 1
3
9
111
TEMPERATURE
TIME

Fig 4

Fig 5.

ORIGINAL PAGE IS
OF POOR QUALITY

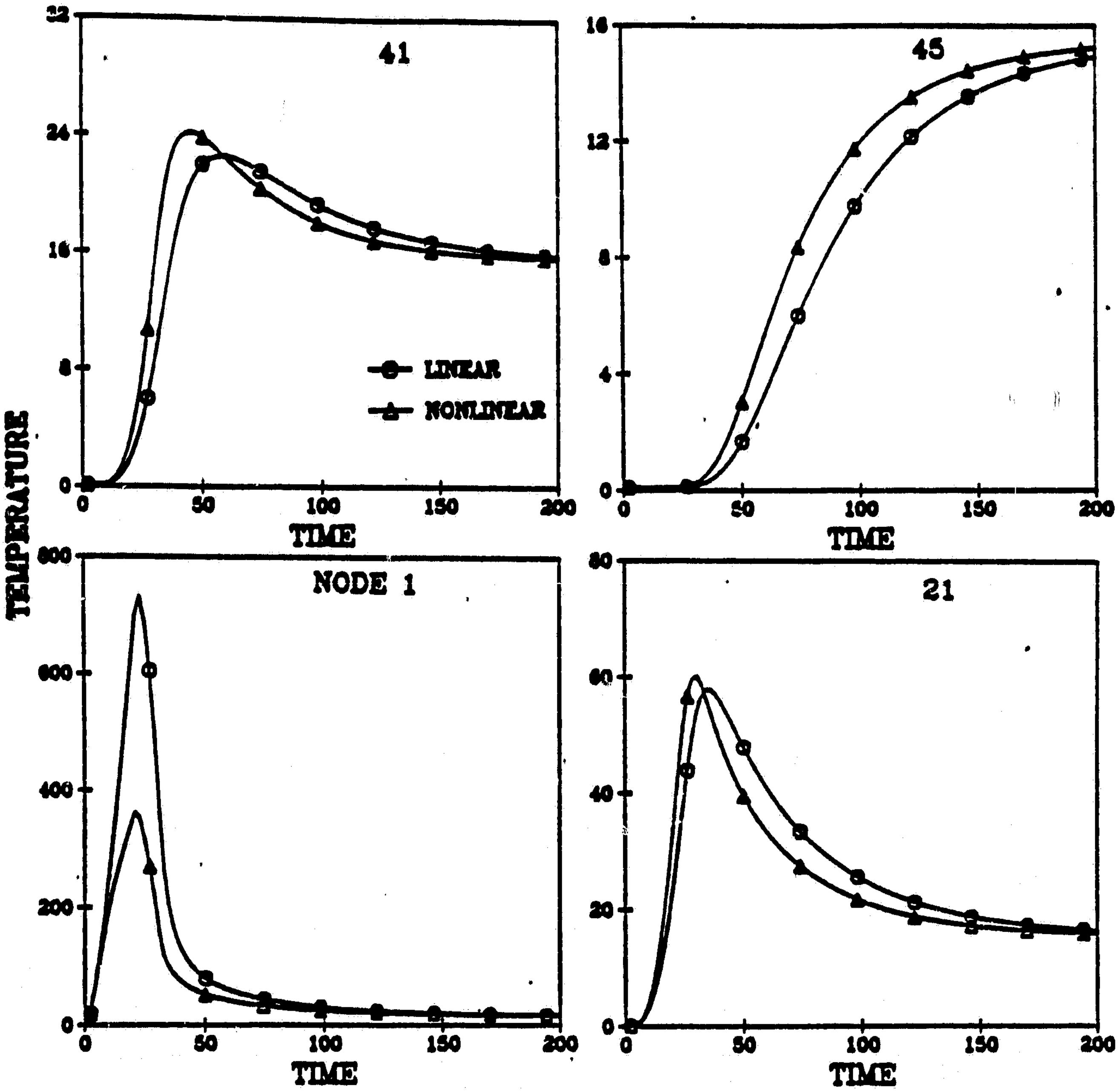

Fig 5a

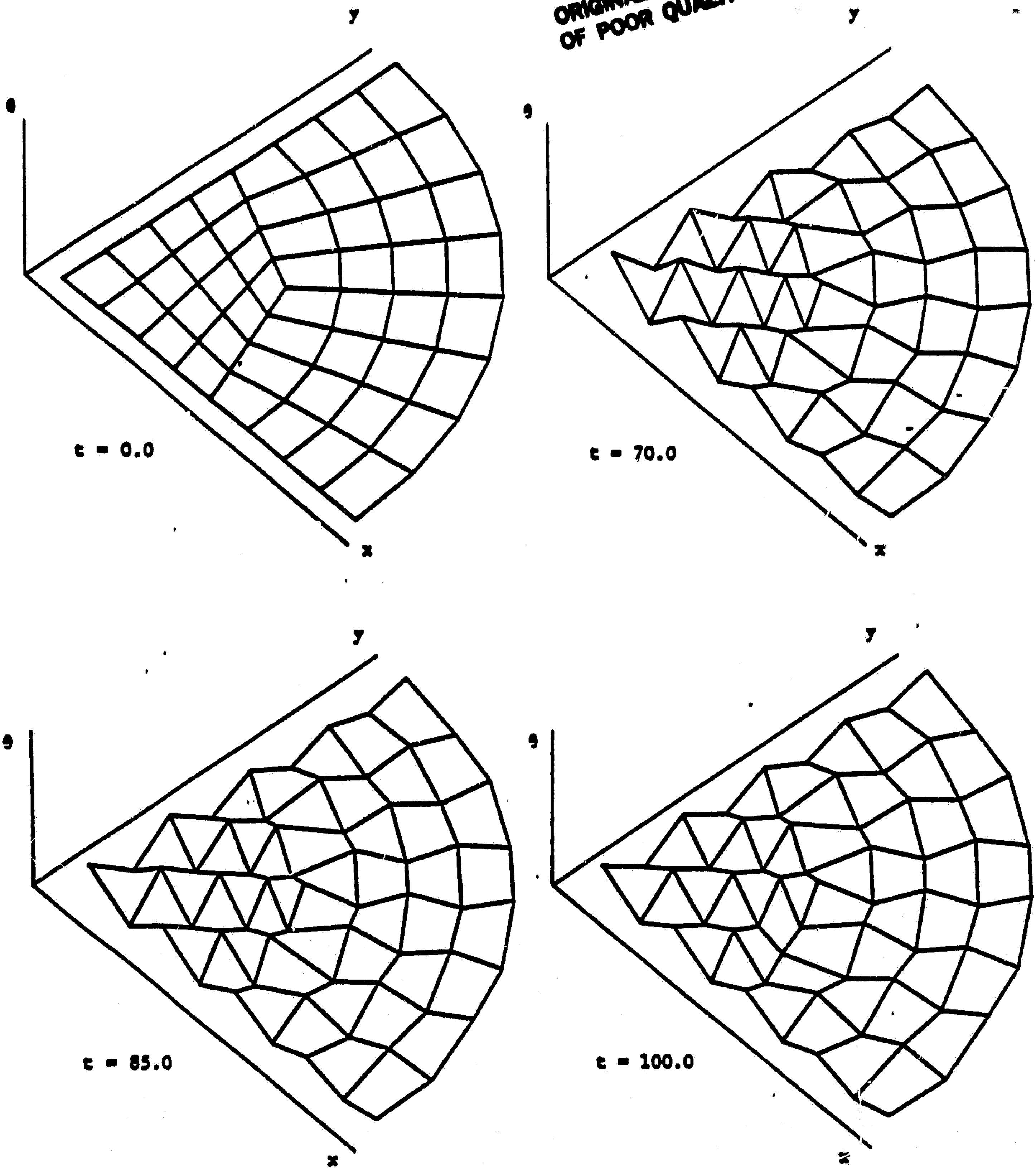

Fig. 5a